npj | precision oncology

Article

Published in partnership with The Hormel Institute, University of Minnesota

https://doi.org/10.1038/s41698-026-01469-z

Dissecting non-small cell lung cancer (NSCLC) with blood proteomics—from surgical to immunotherapeutic responses

Check for updates

Vahid Yaghoubi Naei[1,2,11], Aaron Kilgallon[2,3,11], Gwendoline Mendes[4], Akila Wijerathna-Yapa[2], Sanjay Dutta[5], Clara Lawler[2], Connor O'Leary[5], William Mullally[5], James Monkman[2], James Mansfield[6], Julien Hedou[4,7], Mark N. Adams[8], Ken O'Byrne[5,8], Majid E. Warkiani[9,10] & Arutha Kulasinghe[2,3] ✉

NSCLC remains a leading cause of cancer-related mortality, with limited biomarkers to guide surgical and immunotherapeutic intervention. This study leveraged two complementary plasma proteomics platforms, SomaScan (7596 proteins) and NULISA (250 inflammation-related proteins) to profile 87 timepoints from 56 NSCLC patients, collected pre- and post-surgery and pre- and post-ICI therapy. Robust biomarker selection used adaptive Lasso regression and the Stabl algorithm, with inter- and intra-cohort validation via orthogonal nELISA proteomics. Twenty-one differentially detectable plasma proteins were identified across treatment contexts. Surgical resection induced measurable proteomic changes: non-recurrent patients had higher circulating MUC16 and lower IL36G post-surgery, while recurrent patients showed elevated COX7A2L, FGF19, and SPOCK2, alongside lower FCER2, FCRLA, and SLITRK2. Among ICI-treated patients, responders had lower baseline levels of IL-6, CCL19, IL-2RA, CD200R1, CRP, LIF, PDCD1, CCL7, and SPP1, implicating systemic inflammation and immune regulation in treatment sensitivity. CEACAM5, PTX3, FGF23, and AREG were elevated in patients with worse clinical outcomes and poorer overall survival. MUC16, IL36G, CCL19, and IL-6 were independently validated by nELISA. Cross-platform comparison highlighted the complementary strengths of SomaScan's broad proteomic coverage and NULISA's sensitivity for low-abundance proteins. This integrated approach reveals distinct plasma signatures associated with surgical recurrence, ICI response, and prognosis in NSCLC.

Lung cancer, in particular non-small cell lung cancer (NSCLC), remains among the leading causes of cancer-related deaths worldwide and is the second most frequently diagnosed cancer[1,2]. Detecting lung cancer at an early stage is a critical need to improve therapeutic options and long-term health outcomes[3]. However, NSCLC, the most common form of lung cancer, is often identified at advanced stages, where patient prognosis is often poor. Currently, low-dose computed tomography (LDCT) screening of high-risk individuals (like heavy smokers) can identify early-stage lung cancers and has been shown to reduce lung cancer mortality[4]. However, LDCT's impact is limited by significant drawbacks: screening yields a high rate of false positives (especially in older ages), leading to higher costs and patient anxiety[5]. Additionally, overdiagnosis of indolent lesions and cumulative radiation exposure pose ongoing concerns[6]. These limitations indicate the importance of better non-invasive diagnostic tools, where plasma proteomics offers a means to identify changes in blood detectable proteins to assist early diagnosis, prognostication, and response to therapy

[1]School of Biomedical Engineering, University of Technology Sydney, Sydney, NSW, Australia. [2]Frazer Institute, Faculty of Health, Medicine and Behavioural Sciences, The University of Queensland, Brisbane, QLD, Australia. [3]Queensland Spatial Biology Centre, Wesley Research Institute, The Wesley Hospital, Brisbane, QLD, Australia. [4]SurgeCare SAS, Illkirch-Graffenstaden, France. [5]The Princess Alexandra Hospital, Brisbane, QLD, Australia. [6]Standard BioTools Canada Inc, Markham, ON, Canada. [7]Sorbonne Université, INSERM, Centre de Recherche Saint-Antoine, CRSA, Paris, France. [8]Queensland University of Technology, Brisbane, QLD, Australia. [9]Department of Mechanical Engineering, College of Engineering, American University of Sharjah, Sharjah, United Arab Emirates. [10]The Advanced Biosciences and Bioengineering Research Center, American University of Sharjah, Sharjah, United Arab Emirates. [11]These authors contributed equally: Vahid Yaghoubi Naei, Aaron Kilgallon.
✉e-mail: arutha.kulasinghe@uq.edu.au

The Hormel Institute
University of Minnesota

monitoring[7]. The plasma proteome encompasses a wide range of proteins with different concentrations, reflecting a dynamic state of blood biomarkers, and can be a good proxy for determining tumour states[8]. A recent study identified a panel of three plasma proteins: C-X-C motif chemokine 17 (CXCL17), carcinoembryonic antigen-related cell adhesion molecule 5 (CEACAM5), and WAP four-disulphide core domain protein 2 (WFDC2) that can predict NSCLC risk up to 10 years before diagnosis (achieving ≈0.90 area under the curve (AUC)[9]. Likewise, longitudinal proteomic analyses in NSCLC patients receiving therapy have linked changes in specific plasma proteins to treatment responses. Fold changes in plasma PD-1 during immune checkpoint inhibitor therapy have been shown to correlate with tumour PD-L1 expression and improved patient outcomes[10]. These advances highlight the advantages of plasma proteomics as a complementary strategy to LDCT, with the potential to improve early NSCLC diagnosis and to enable proactive treatment response monitoring for better clinical management[11].

Precise and unbiased affinity-based methods for large-scale proteome analysis, like SomaScan (SomaLogic, US), Nucleic Acid-Linked Immuno-Sandwich Assay (NULISA) (Alamar Biosciences, US), and next-generation Enzyme-Linked Immunosorbent Assays (nELISA) (Nomic Bio, Canada), have been recently developed, demonstrating high sensitivity and specificity for a wide array of proteins across the entire dynamic range in complex fluids, like serum or plasma. These advancements address the limitations of traditional and even complex mass spectrometry technologies in detecting new disease biomarkers[12,13]. In this study, we aim to investigate the plasma proteomes of NSCLC patients using SomaScan v4.1, which comprises reagents to detect 7596 plasma proteins including cardiovascular, inflammation and immune response, metabolic diseases, oncology, neurology, cytokines, and respiratory disease biomarkers, and the NULISA Inflammation Panel, which detects 250 proteins, before and after surgery, and before and after immune checkpoint immunotherapy, to discover potential prognostic and diagnostic biomarkers. We utilised the feature selection method Stabl in combination with linear modelling to identify protein signatures associated with plasma proteome changes induced by adjuvant surgery, proteins associated with disease recurrence, proteins prognosticative of response to immunotherapy, and proteins associated with patient survival[14].

To address the critical need for biomarker validation and to overcome platform-specific biases, we employed a multi-platform validation strategy. Following discovery using SomaScan and NULISA panels, we validated key findings in inter- and intra- cohort using nELISA, which provides orthogonal antibody-based quantification. This approach addresses concerns about reproducibility and establishes the robustness of identified biomarker signatures across different proteomic technologies.

Results

Correlating protein signatures across platforms

An overview of the patient cohorts in this study is shown in Fig. 1. To evaluate the consistency of protein measurements across technologies, we performed a cross-platform correlation analysis of matched pre- and post-surgery samples. This approach enabled us to identify overlapping protein signals and assess accordance between the SomaScan and NULISA platforms. Cross-platform analysis of the pre- and post-surgery samples identified a cluster of highly correlated proteins that. Amongst them, chemokines C-C motif chemokine ligand 28 (CCL28), C-X-C motif chemokine ligand 2 (CXCL2; also known as GROβ or MIP-2α), C-C motif chemokine ligand 17 (CCL17; also known as Thymus and activation-regulated chemokine), C-C motif chemokine ligand 5 (CCL5; commonly known as Regulated upon Activation, Normal T cell Expressed and Secreted/RANTES), matrix remodelling enzymes (MMP1), angiogenic factors Platelet Derived Growth Factor Subunit A (PDGFA), Platelet Derived Growth Factor Subunit B (PDGFB), Angiopoietin 1 (ANGPT1), and the neuroimmune modulator Brain-derived neurotrophic factor exhibited strong correlations between the SomaScan and NULISA platforms, as shown in Fig. 2.

Surgery-induced alterations in the plasma proteome

Matched patient samples pre- and post-surgery revealed measurable changes in protein expression. The predictive models constructed using proteins ($n = 17$ patients) selected by ALasso and Stabl including inflammatory markers Interleukin-36 gamma (IL36G), epithelial associated proteins (MUC16), and extracellular matrix proteins Thrombospondin 3 (THBS3), C-type lectin domain family 3 member B (CLEC3B; also known as Tetranectin), and Transforming growth factor-beta-induced (TGFBI), demonstrated strong performance with an AUROC of 0.81 for ALasso (Fig. 3A) and 0.76 for Stabl (Fig. 3C). The fold change plot generated with the NULISA assay highlighted an opposing trend in the expression of two key markers: Mucin-16 (MUC16) was upregulated after surgery, whereas IL36G was downregulated ($P = 0.01$). The reduction of IL36G, a pro-inflammatory cytokine, may indicate attenuation of systemic inflammatory signalling following tumour resection, while the post-surgical increase in circulating MUC16 suggests persistent epithelial or tumour-associated protein release. These markers were consistently identified by both feature selection methods (ALasso and Stabl) as leading predictors distinguishing pre- and post-surgical states (Fig. 3B, D). From the SomaScan assay using both selection models (Fig. 3E, G), Thrombospondin-3 (THBS3), Tetranectin (CLEC3B), KxDL motif-containing protein 1 (KDXI), SHC-transforming protein 1 (SHC1), and TGFBI were identified as differentially expressed markers ($n = 20$ patients). Differential expression box plots indicated a reduction for CLEC3B, TGFBI, and KDXI, but an increase for THBS3 and SHC1 in post-surgery samples (Fig. 3F, H). Notably, several of these proteins are functionally associated with extracellular matrix organisation, tissue remodelling, and cellular stress responses, suggesting that the observed expression shifts are biologically consistent with postoperative wound healing and tissue adaptation processes. On both platforms, MUC16, IL36G, THBS3, CLEC3B, and TGFBI were chosen by both selection methods. Comparing the NULISA assay with SomaScan protein expression in a univariate analysis revealed that the former had a higher statistical limit for detecting log-fold changes in protein expression, mainly due to its higher sensitivity (Fig. 3I). Pathway enrichment analysis of the selected proteins highlighted key biological processes affected by surgery, including cytokine activity ($P = 0.0093$) and signalling ($P = 0.031$), extracellular compartments ($P = 2.46e-06$), and cytokine–cytokine receptor interaction ($P = 0.0016$).

Plasma proteomic changes associated with post-surgical NSCLC tumour recurrence

Comparative analysis of feature selection performed on NULISA and SomaScan data independently using Stabl and ALasso methods showed recurrence-related changes in plasma proteins that only reached statistical significance when using ALasso selection on pre-surgical samples ($P = 0.015$, AUROC = 0.85) on the SomaScan panel (Fig. 4A). Higher expression of mitochondrial cytochrome c oxidase subunit 7A2-like (COX7A2L), fibroblast growth factor 19 (FGF19), and Testican-2 (SPOCK2) was seen in NSCLC patients with tumour recurrence. Conversely, the low-affinity immunoglobulin epsilon Fc receptor (FCER2), Fc receptor-like A (FCRLA), and SLIT and NTRK-like protein 2 (SLITRK2) had lower expression in recurrent versus non-recurrent cases (Fig. 4b, d), consistent with a relative suppression of immune-associated signatures in these patients, potentially reflecting a less immunologically active systemic environment in those prone to disease progression.

Although Stabl did not detect statistically significant features ($P = 0.062$, AUROC = 0.77), FCER2, SPOCK2 and COX7A2L markers were similarly selected by this method (Fig. 4C), supporting the robustness of these signals across modelling approaches. We therefore used these features as probes for pathway enrichment associated with these markers. Pathway enrichment analysis revealed significant involvement of the identified markers in lymph node development ($P = 0.0013$), positive regulation of lymphocytes ($P = 0.00097$), cytokine–cytokine receptor interaction ($P = 4.27e-10$), and TNF receptor superfamily signalling ($P = 0.0016$),

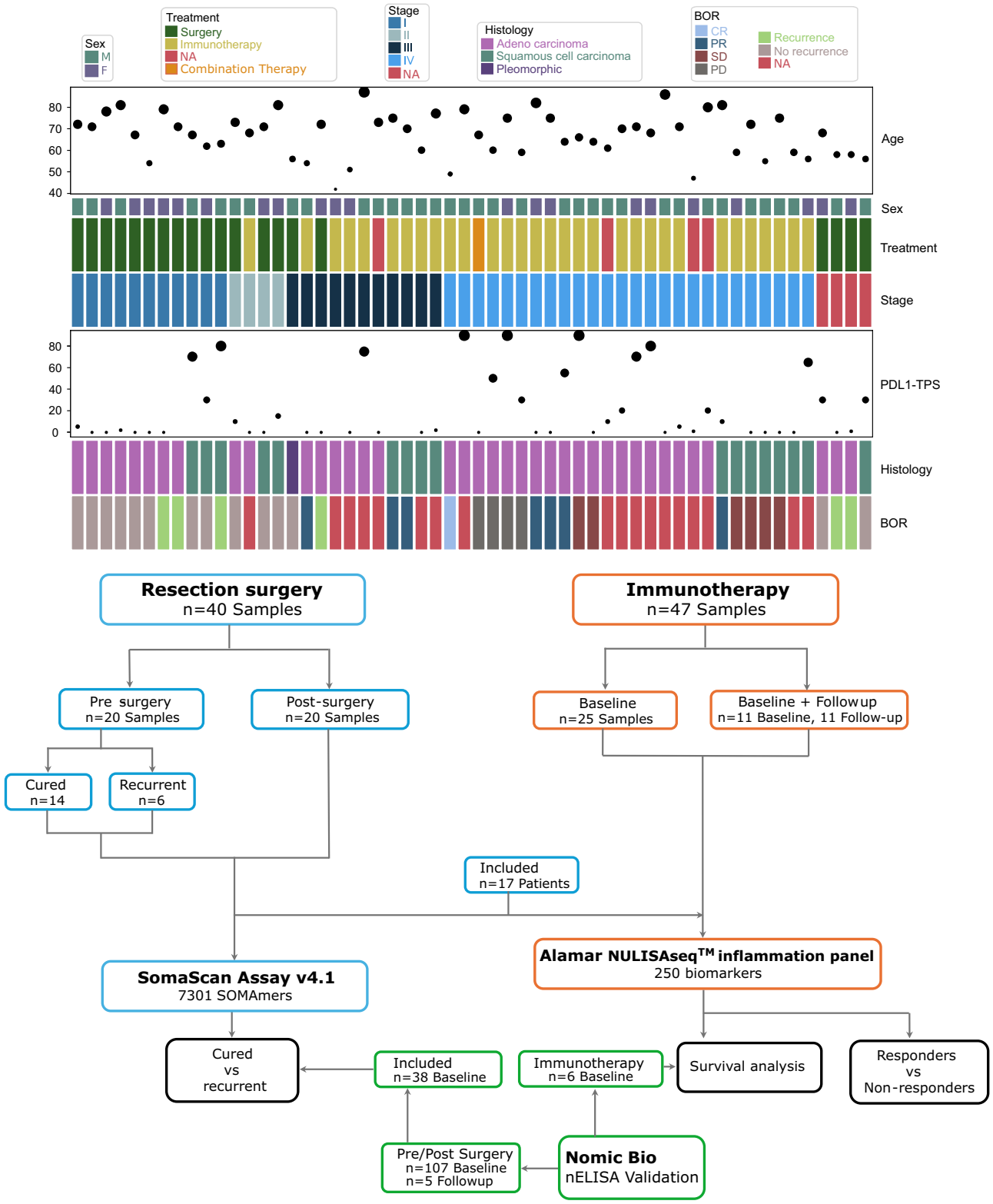

Fig. 1 | Patient clinical information chart showing age, sex, treatment mode, stage of the disease, PDL1 tumour proportion score, histology subtype and best overall response to therapy (top). Comparison of 20 NSCLC patient samples at two time points (pre- and post-resection surgery), cured vs. recurrent, using the SomaScan assay. Comparison of the plasma profiles of 25 baseline immunotherapy patient samples and pre- and post-immunotherapy plasma profiles for 11 patients using the NULISA panel(bottom). N number of patients. The size of dots in the Age and PDL1-TPS panels is scaled by their plotted values to aid in interpretation.

indicating that immune regulatory pathways are a prominent component of the biological differences observed between recurrent and non-recurrent cases. However, due to the limited validation cohort size, these represent discovery findings requiring future validation.

Plasma proteomic signatures pre/post immunotherapy

To identify plasma protein markers associated with immunotherapy response, we profiled 30 plasma samples collected from NSCLC patients before initiation of immunotherapy using the NULISA assay. Patients were

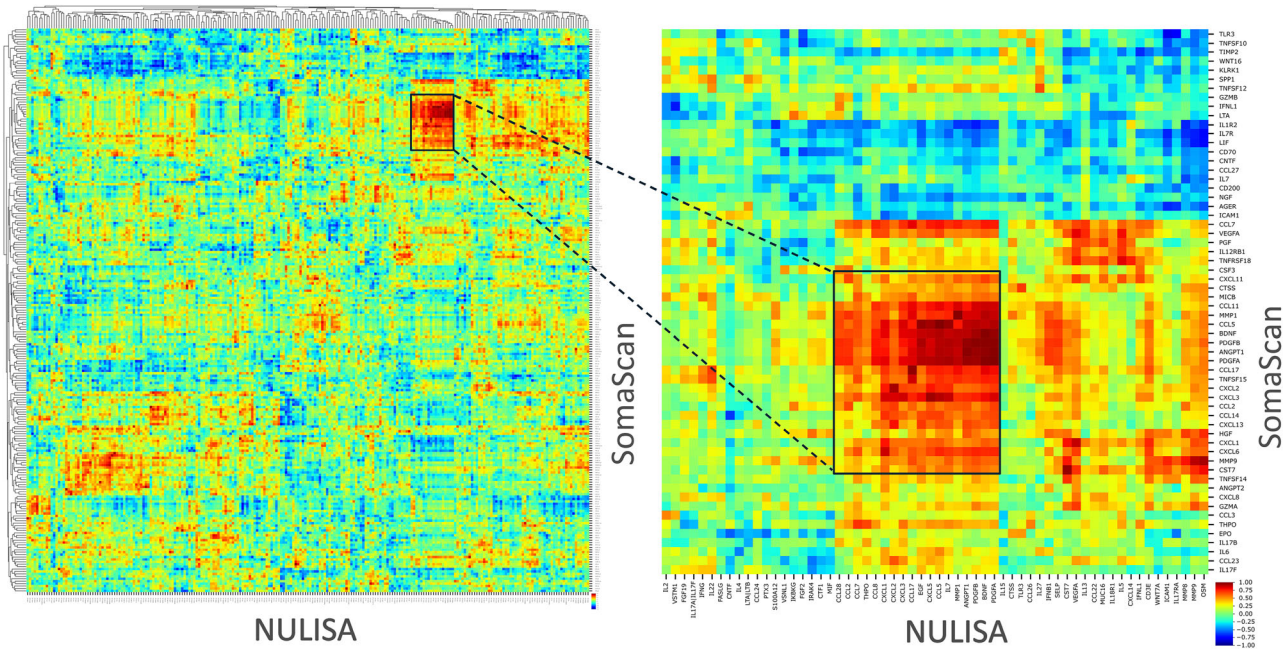

Fig. 2 | A heatmap illustrating the cross-platform correlation of overlapping proteins identified through SomaScan and NULISA panels. The left panel presents the complete correlation heatmap, showing correlations in global expression patterns across both platforms in response to surgical intervention. The right panel presents a magnified view of the clustered region that includes strongly correlated markers.

categorised as responders (complete response (CR), partial response (PR)) or non-responders (stable disease (SD), progressive disease (PD)) based on their RECIST criteria. Associated proteins were identified through the two feature selection methods applied separately to data from each assay, which yielded five markers with strong selection signals and statistically significant *P*-values ($P = 0.012$, AUROC = 0.83) (Fig. 5A). Among those, Interleukin-2 receptor subunit alpha (IL-2RA), Interleukin-6 (IL-6), C-reactive protein (CRP), C-C motif chemokine 7 (CCL7) and C-C motif chemokine 19 (CCL19) are well-recognised for their roles in pro-inflammatory and immune activation processes[15]. Cell surface glycoprotein CD200 receptor 1 (CD200R1) is associated with immune regulation, Osteopontin (SPP1) is typically produced in response to inflammation, and programmed cell death protein 1 (PDCD1), C-type lectin domain family 4 member A (CLEC4A), and Leukaemia inhibitory factor (LIF) were identified, several of which are functionally linked to immune regulation and immunosuppressive signalling[16]. Univariate analysis and differential expression box plots showed that all highlighted markers were downregulated in responders except CLEC4A (Fig. 5B, C), indicating that patients who benefited from immunotherapy exhibited globally lower baseline levels of circulating inflammatory, chemokine, and immune-regulatory mediators compared with non-responders. This pattern suggests that a pre-existing state of heightened systemic inflammation or immune dysregulation may be associated with reduced therapeutic benefit. According to KEGG, STRING, and Reactome databases, these markers are significantly enriched in pathways related to cell migration ($P = 0.0032$), inflammatory response ($P = 0.00064$), chemokine signalling ($P = 5.80e\text{-}05$), and IL-6 family signalling ($P = 0.042$), highlighting that the identified baseline plasma proteins collectively capture an immune-inflammatory landscape that is biologically relevant to treatment responsiveness rather than isolated single-marker effects.

A subset of 11 patients with both baseline and follow-up plasma samples, collected 3–6 months (median follow-up time: 4.5 months) after immunotherapy, were analysed. This longitudinal analysis was performed on all patients with paired pre- and post-immunotherapy samples, independent of response group, to explore dynamic treatment-associated changes in circulating proteins over time. Despite achieving a high AUROC, neither analysis model reached statistical significance due to the small sample size ($P = 0.12$, AUROC = 0.80). Six markers of treatment outcome, including C-C motif chemokine 21 (CCL21), CD276 antigen (B7-H3), IL-2RA, and Interleukin-24 (IL-24), Interleukin 1 receptor-like 1 (IL-1RL1) and Receptor for Advanced Glycation End-products or AGER, were identified by both models (Fig. 5D). A number of these proteins participate in immune trafficking, checkpoint regulation, and inflammatory signalling, suggesting that longitudinal variations in circulating immune mediators may correlate with response dynamics.

Survival outcomes following immunotherapy

Survival analysis was performed on samples from 36 immunotherapy-treated patients using a regularised Cox Proportional Hazards model, with proteins initially selected via ALasso. This approach identified nine differentially expressed markers, yielding a concordance index of 0.54 (Fig. 6A). Stabl validation refined this selection to four key proteins, substantially improving model performance (concordance index = 0.80) when feature selection was based on a CoxPH model fitted to censored progression-free survival time. Their elevated baseline levels were negatively correlated with patient survival, indicating that higher circulating concentrations of these proteins predict poorer outcomes following immunotherapy ($P = 0.073$) (Fig. 6B). The four selected proteins (Fig. 6C) were: the cell adhesion molecule CEACAM5 (hazard ratio (logHR) = 0.18), pentraxin-related protein PTX3 (logHR = 0.065), fibroblast growth factor 23 (FGF23) (logHR = 0.077), and amphiregulin (AREG) (logHR = 0.31). Pathway analyses revealed enrichment in proteins associated with MAPK1/MAPK3 signalling ($P = 0.0197$) and the interleukin-6 receptor alpha chain (suggesting that the identified survival-associated markers converge on signalling pathways linked to inflammation, growth-factor signalling, and immune modulation.

We sought to validate these proteins in patients using an orthogonal protein panel using the Nomics Bio nELISA platform. Within matched samples from the primary cohort profiled using this panel, we found significant changes ($P = 0.006$) in MUC16 pre- and post- surgery (Fig. 7A). We examined an external cohort of 107 pre-surgical resection-treated samples and 5 follow-up samples, for overlapping circulating proteins quantified using the nELISA panel. Within this external cohort, we validated the significant changes ($P = 0.021$) in IL-36G (Fig. 7B) induced by surgical

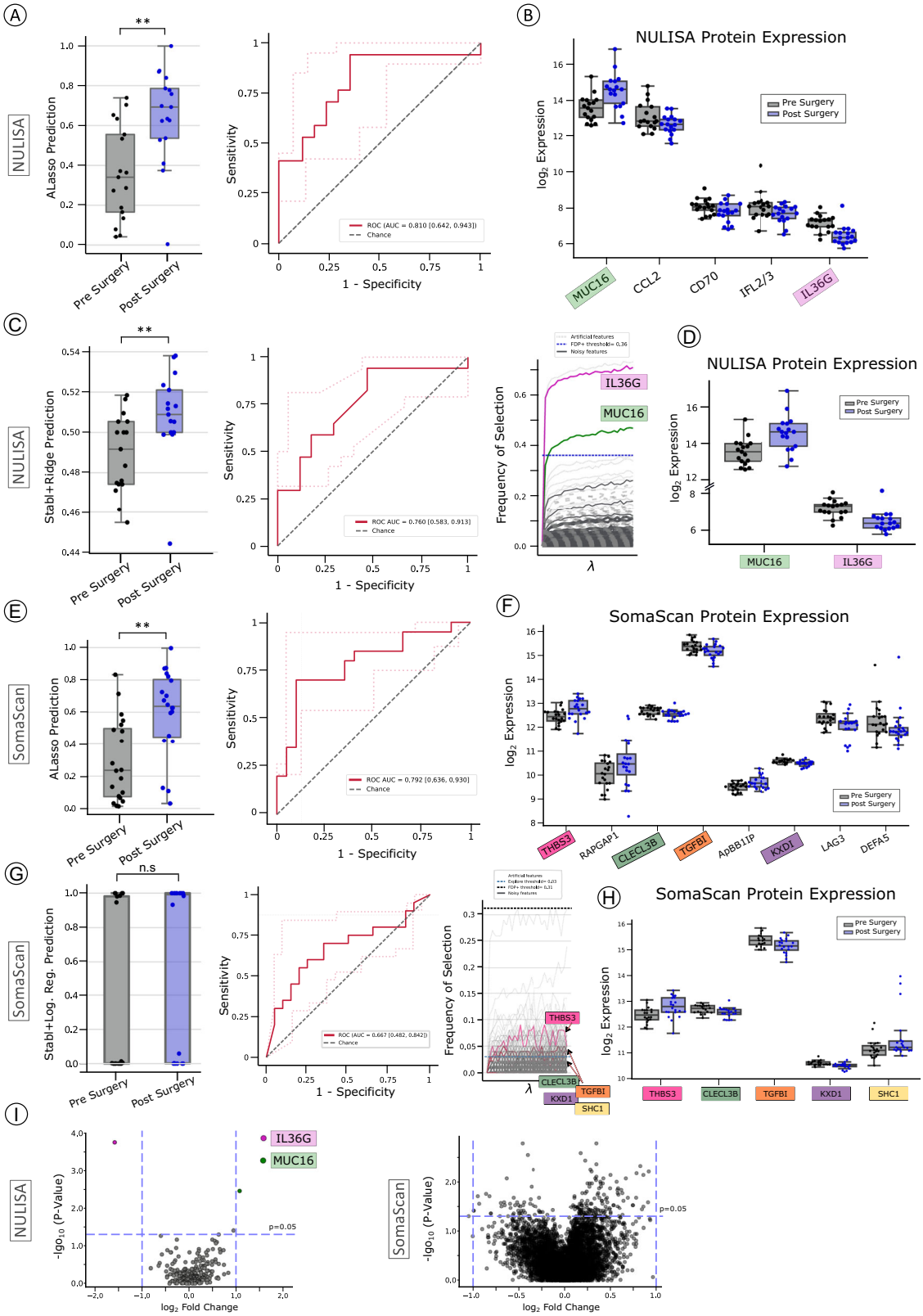

Fig. 3 | Comparative analysis of pre- and post-surgery plasma proteomics. A Box plots of Adaptive Lasso model predictions (left) and corresponding ROC curves (right) of selected proteins from the NULISA panel ($P = 0.002$). **B** Expression values of selected proteins of the Adaptive Lasso model using NULISA data. **C** Box plots of Stabl+Ridge Regression model predictions (left), corresponding ROC curves (middle), and Stabl regularisation paths (right) for selected proteins from NULISA data ($P = 0.01$). **D** Expression of Stabl-selection proteins using NULISA data. **E** Box plots of model predictions (left), corresponding ROC curves (right) for proteins selected by Adaptive Lasso feature selection on SomaScan data ($P = 0.001$). **F** Expression values of selected proteins of the Adaptive Lasso model using the SomaScan data. **G** Box plots of Stabl+Logistic Regression model predictions (left), corresponding ROC curves (middle), and Stabl regularisation paths (right) for selected proteins from the SomaScan panel. **H** Expressions of selection proteins using SomaScan data. **I** Univariate analysis of NULISA protein expression (left) and SomaScan protein expression (right) shows the comparative advantage of the high-sensitivity NULISA assay in detecting significant log-fold changes in protein expression.

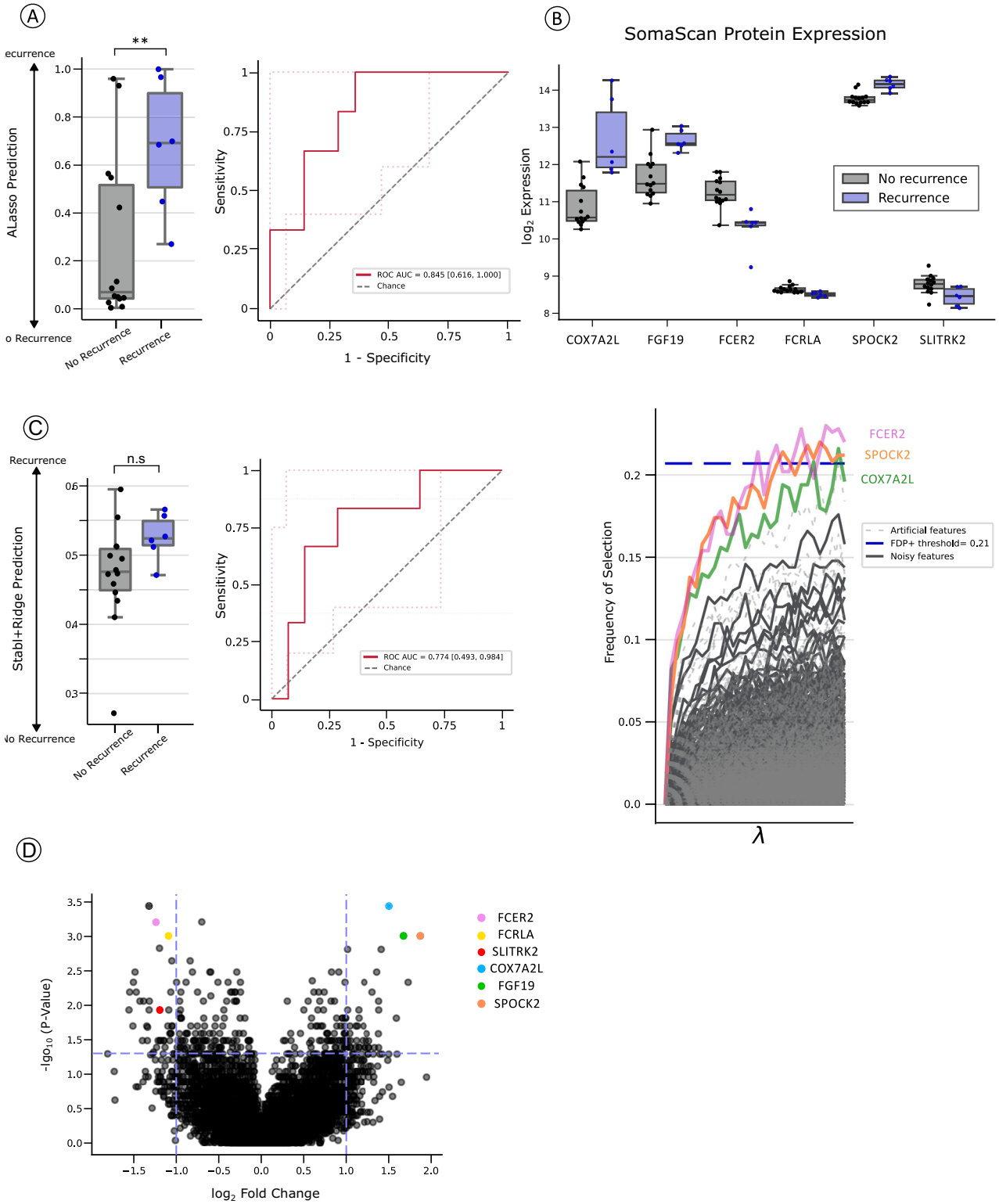

Fig. 4 | Comparative analysis of post-surgery plasma proteomic profiles of recurrent patients against non-recurrent patients. A Box plots of model predictions (left) and corresponding ROC curves (right) for proteins selected using Adaptive Lasso ($P = 0.015$). **B** Expression values of proteins selected by the Adaptive Lasso model using SomaScan data. **C** Box plots of Stabl+Ridge regression model predictions (left), corresponding ROC curves (middle), and Stabl regularisation paths using SomaScan data (right). **D** Log-fold changes in the SomaScan assay show that a number of univariate statistically significant proteins were selected as informative by the Adaptive Lasso selection method.

resection. We additionally examined the profiles across responders and non-responders for the combined inter- and intra-cohort but found limited statistical power to fully validate the proteins given the correlation between these panels (Fig. 7D).

We then augmented the primary patient cohort with 6 additional baseline measurements taken from NSCLC patients treated with immunotherapy agents. The combined cohort prevented grouping by RECIST scores (Fig. 7C), however, this combined cohort was examined for significant

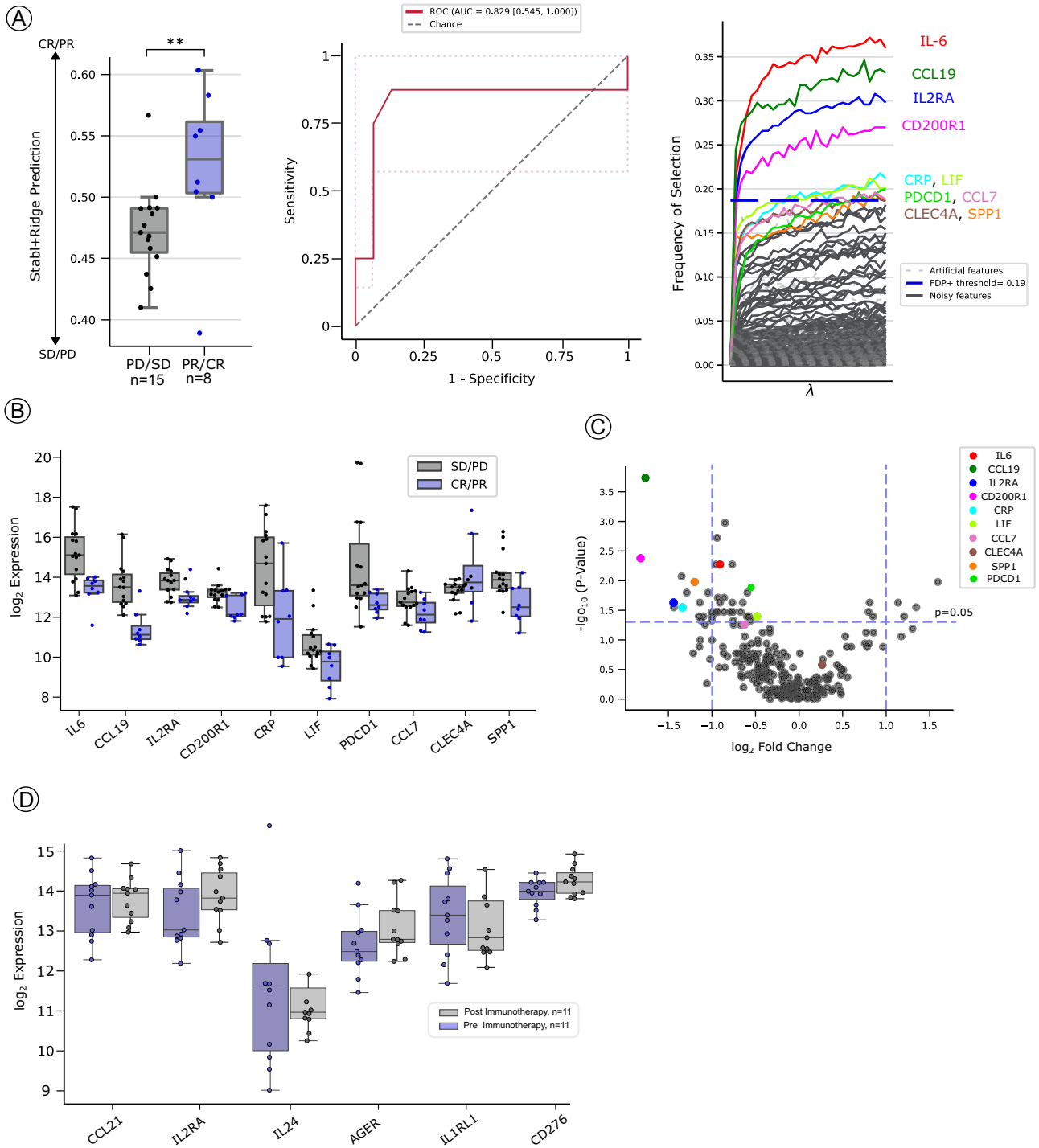

Fig. 5 | Comparative analysis of baseline immunotherapy plasma proteomic profiles using the NULISA platform to distinguish clinical response groups. **A** Box plots of model predictions (left), corresponding ROC curves (middle), and Stabl regularisation paths (right) for distinguishing responders vs. non-responders samples using NULISA data ($P = 0.012$). **B** Expressions values of selected proteins of the Stabl with Ridge regression model for distinguishing responders vs. non-responders using NULISA data. **C** Univariate analysis of log-fold differences in protein expression of selected proteins from the NULISA data. **D** Expression values of selected proteins of the Adaptive Lasso and Stabl models for comparing differential expressions before and after ICI therapy using the NULISA data.

features associated with response to immunotherapy treatments using a Cox Proportional Hazards analysis to leverage the informative nature of time-to-event data. Hazard ratios of protein measurements were evaluated relative to age, sex, and histology (adenocarcinoma yes/no) as covariates to model overall survival or progression-free survival (Supplementary Tables 2 and 3). Of the 6 overlapping selected proteins between the nELISA and the NULISA panels, IL-6 was significant (HR = 2.24 [1.12, 4.5]) and CCL19 was significant (HR = 1.81 [1.04, 3.17]) for overall survival (24 patients, 14 observed events). We examined the correlation between marker measurements in the surgical baseline samples, finding poor correlation between these panel measurements (Fig. 7E), giving indications as to why only a subset of these protein measurements extrapolated into an orthogonal panel.

Confounder analysis

We evaluated the impact of clinical variables on the model's performance, including PD-L1 tumour proportion score (TPS), overall survival, disease

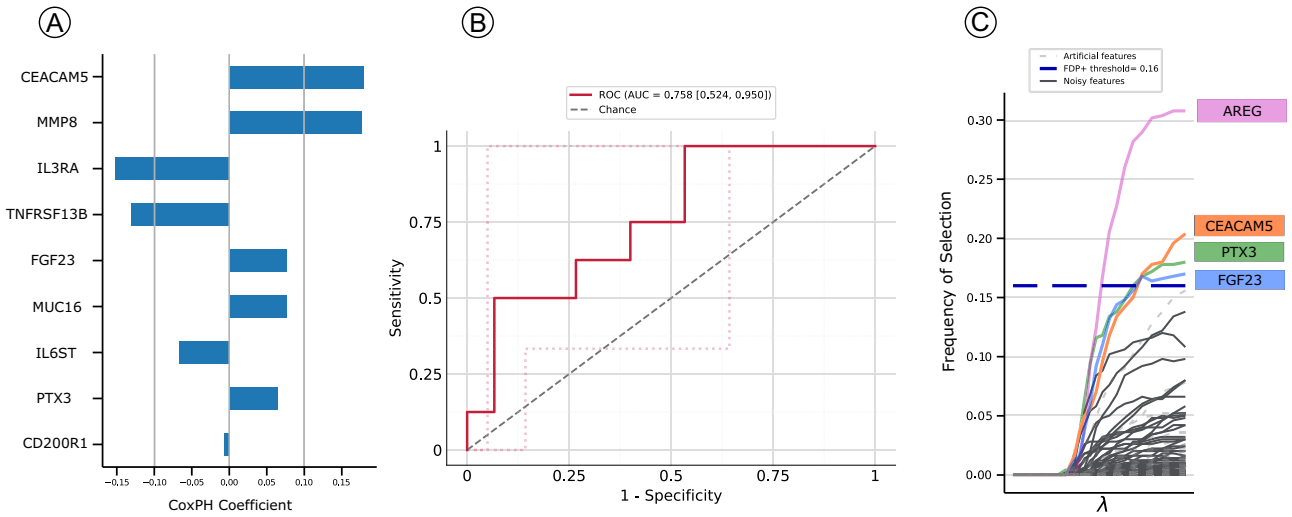

Fig. 6 | Survival analysis of plasma proteomic profiles selected from the NULISA panel using ALasso and Stabl feature selection methods. A Cox model for markers selected using ALasso to predict survival endpoints. **B** ROC curve demonstrating the predictive performance of the Stabl model in selecting 4 key NULISA markers that can model grouped patient response. **C** Regularisation paths of NULISA proteins selected by the Stabl model to differentiate survival endpoints.

stage, survival status, metastasis location, as well as different treatment modalities, such as chemotherapy, immunotherapy, and targeted therapy. To evaluate the independence of our proteomic signature, we integrated the models' predictions as continuous scores into multivariable regression models alongside the clinical covariates. While disease stage was a significant predictor ($P = 0.047$) in predicting immunotherapy response, the proteomic signature remained independently associated with the outcome, with no drop in AUC upon the addition of this or other clinical variables (Supplementary Table 1). This demonstrates that the proteomic signal captures predictive information not accounted for by standard clinical staging. This finding underscores the importance of considering disease stage as a factor when deriving prognostic models using plasma proteins in immunotherapy-treated patients; despite the proteomic signature's independence from the clinical stage, this model was marginally benefited by the complementary staging information.

Discussion

Blood proteomic biomarkers offer a real-time and non-invasive way to capture dynamic tumour and immune-related signals to better guide disease stratification and therapeutic outcomes for surgery and targeted therapies. We profiled the plasma proteome of 56 NSCLC patients covering various clinical modalities, including before and after lung resection surgery, recurrent versus non-recurrent post-surgery, and pre- versus post-immunotherapy. Our analysis used two plasma proteomics platforms, NULISA and SomaScan, in primary analysis, with validation using the nELISA platform. By applying false discovery-corrected feature-selection methods, we identified distinct protein signatures associated with different clinical groups, including surgical, recurrence, and ICI therapy, and validated a subset of these in a complementary set of patient measurements.

NULISA employs a highly sensitive dual-antibody sandwich approach with DNA barcoding and NGS, achieving attomolar sensitivity by significantly reducing background signal. Being highly sensitive enables this platform to detect low-abundance proteins like cytokines and immune regulators using a smaller panel of 250 probes. In contrast, SomaScan uses aptamer technology, where numerous oligonucleotide probes cover 7596 proteins with high throughput. These differences can lead to variability in protein detection between the two platforms, where aptamer and antibody-based assays may indicate variable correlations depending on target characteristics[17]. SomaScan's broader coverage facilitated the detection of a diverse array of proteins, including those involved in extracellular matrix remodelling and metabolic regulation. Our direct comparison of these platforms highlights their complementary strengths and specific instances where their detection capabilities vary. The notable cross-platform correlation emphasises the robustness and reproducibility of our findings, pointing to that both platforms effectively capture comparable biological variations, despite differences in technology, scale of measurements, and panel focus. In overlapping regions of the two protein panels, correlation of essential immune, vascular, and tissue remodelling markers was found across the two independent proteomic platforms. These include chemokines that facilitate immune cell recruitment (CCL28, CCL17, CXCL2, CCL5), as well as mediators involved in extracellular matrix remodelling (MMP1) and angiogenesis (PDGFA, PDGFB, ANGPT1). These variations have noticeable implications for biomarker discovery and interpretation, emphasising the importance of understanding platform-specific characteristics when selecting biomarkers for translational studies.

Given that the NULISA results were used as the primary basis for biomarker selection in immunotherapy analyses, the existing overlap amongst all three panels, and the limited validation cohort size for immunotherapy and survival endpoints, these analyses remain exploratory and are reported as discovery findings requiring future validation.

Detectable proteins in the blood, such as those involved in inflammation, coagulation factors, and stress hormones, varied between pre-surgery and post-surgery, provide insights into the biological processes associated with surgical intervention. We observed a reduction in IL-36G in post-surgery samples, a pro-inflammatory cytokine known for activating $CD8^+$ T cells and NK cells, which may reflect a dampening of systemic inflammation following tumour removal[18], with validation using the nELISA platform in an independent cohort. Conversely, we found elevated circulating levels of MUC16 after surgery—a glycoprotein expressed on the surface of various epithelial cells, reported to be higher in different types of lung cancer, particularly in advanced stages[19,20], with validation using the nELISA platform within the primary cohort. We observed, post-surgery, downregulation of CLEC3B, KXD1, and TGFBI alongside upregulation of SHC1 and THBS3[21], with pathway analysis results further supporting the critical role of cytokines and extracellular matrix components in distinguishing pre-surgery from post-surgery conditions. Reduction of CLEC3B and TGFBI, both associated with tumour ECM remodelling and tissue homoeostasis, together with reduced KXD1, linked to lysosomal function, may reflect early systemic responses to surgical intervention. In parallel, increased SHC1 and THBS3, which are involved in wound healing, angiogenesis, and ECM remodelling, likely indicate active tissue repair and remodelling processes[22]. These expression changes are consistent with

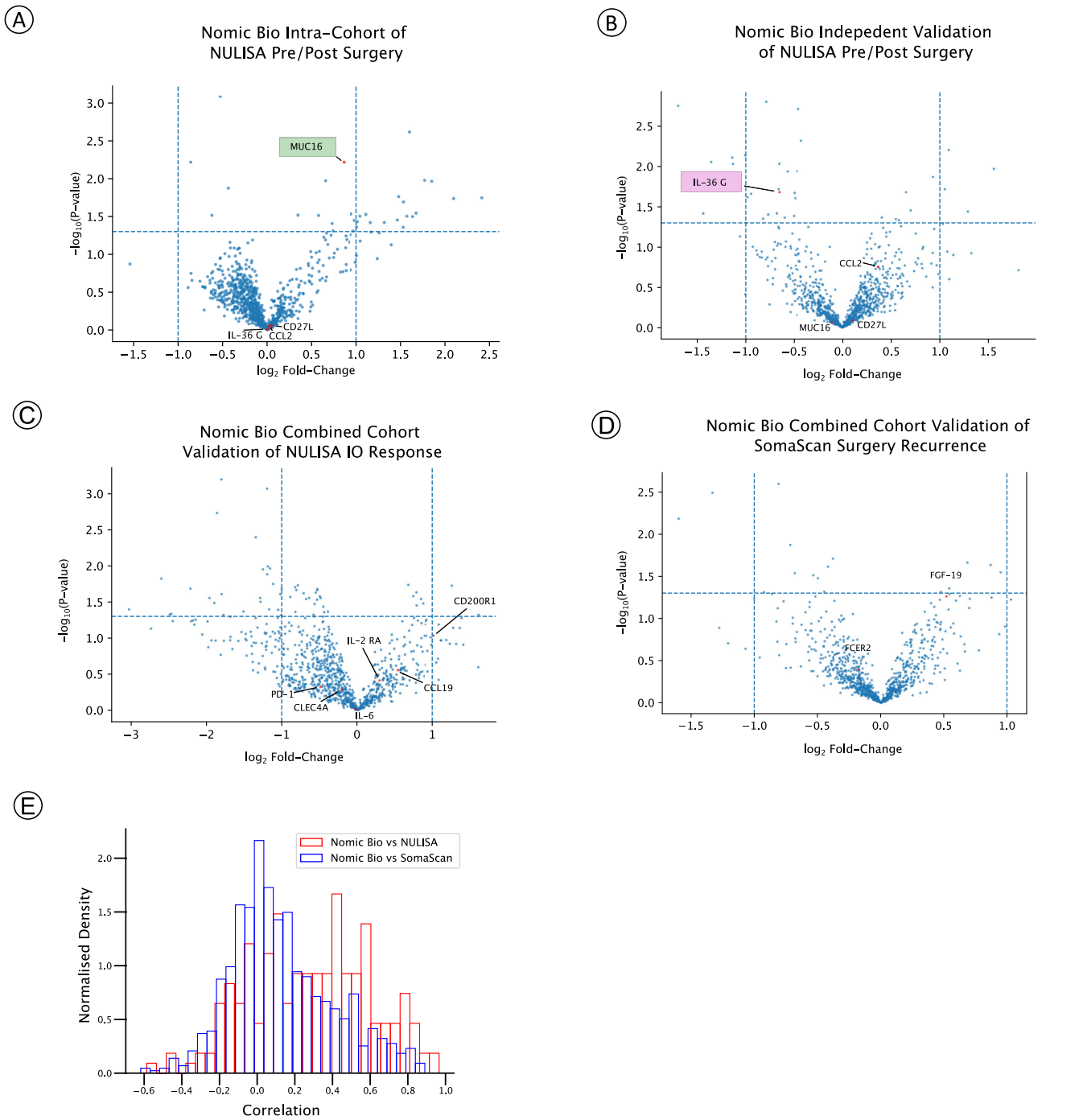

Fig. 7 | Validation of selected proteins in longitudinal surgical and surgical /immunotherapy response results using an orthogonal proteomics panel. **A** Volcano plot of Nomics protein measurements in longitudinal pre- and post-surgical samples ($n = 17$, $n = 14$) for matched patients from the primary cohort, evaluated using *limma*. **B** Volcano plot of Nomics protein measurements in longitudinal pre- and post- surgical samples for an independent cohort ($n = 107$, $n = 5$). **C** Volcano plot of nELISA protein measurements in matched and external patients ($n = 9$ responders, $n = 7$ non-responders) for IO response in the NULISA study. **D** Volcano plot of nELISA protein measurements in baseline surgical samples to predict tumour recurrence (no-recurrence $n = 25$, recurrence $n = 13$). **E** Histogram of Spearman correlation coefficients between Nomics and NULISA/SomaScan measurements.

biological adaptations following surgery and may reflect wound healing and tissue reconstruction dynamics.

NSCLC recurrence rate following surgery remains a clinical challenge, with rates ranging from 15- 20%[23]. Improving postoperative monitoring and treatment strategies depends on the identification of recurrence-associated plasma proteins[24]. We found proteins involved in immune regulation and inflammation (FCER2, FCRLA, and SLITRK2), metabolic adaptation (COX7A2L), cell signalling and growth regulation (FGF19), and extracellular matrix regulation (SPOCK2) associated with tumour recurrence. While no study to date has specifically explored the plasma levels of FCER2, FCRLA, and SLITRK2 in lung cancer following surgery, their higher expression within tumour tissue has been linked to better overall survival, reduced risk of metastasis, and more favourable outcomes. In contrast, we found the opposite trend, with patients who experienced recurrence after surgery having lower levels of these markers compared to those who remained cancer-free. Since COX7A2L participates in the stabilisation of

mitochondrial respiratory supercomplexes, it is expected to decrease in the hypoxic environment of the TME, as reported by Hollinshead et al., who observed reduced mRNA and protein levels in lung cancer cells[25]. Although the role of circulating COX7A2L in post-surgery lung cancer recurrence has not been specifically investigated, we observed higher plasma levels of this marker in patients who experienced tumour recurrence compared to those who remained disease-free. A similar opposite trend between previous tissue studies and our plasma profiling in recurrent cases was also seen for SPOCK2[26]. In contrast, and in line with our plasma findings, Chen et al. reported elevated tissue expression of FGF19 as an independent prognostic indicator for recurrence following NSCLC surgical resection[27].

Immunotherapy has transformed lung cancer care, yet predictors of treatment response remain intangible. We profiled baseline plasma samples from patients prior to ICI therapy and categorised biomarkers according to RECIST-defined responses. Among the markers that were elevated in non-responders (SD/PD) relative to responders (CR/PR), there is supporting prior publications linking IL-6[28], IL-2RA[29], SPP1[30], CD200R1, and CCL19 to systemic inflammation, immune suppression, and/or poor outcomes.

IL-6 is reported to have contrasting effects on immunotherapy. In one cohort of 125 advanced NSCLC patients, low baseline IL-6 (<13.1 pg/mL) was associated with significantly higher objective response and disease control rates and longer PFS/OS under anti-PD-1/PD-L1 therapy[31], in line with our findings. On the other hand, another study found that patients with high IL-6 had poor outcomes (median PFS ~1.9 vs. 6.3 months)[32]. Our finding that circulating IL-2RA is elevated in non-responders confirms the results of a previous study that found high baseline IL-2RA serum levels predicted poor PD-1/PD-L1 therapy response[29]. SSP1 is a pleiotropic secreted protein overexpressed in lung cancer, which promotes tumour growth, metastasis, and creates an immunosuppressive microenvironment[30]. We found that higher baseline SPP1 levels were linked to worse ICI response, which is supported by other studies showing high pre-treatment serum SPP1 correlates with poor clinical response and higher mortality in NSCLC patients treated with nivolumab and pembrolizumab[30].

In addition to these known markers, we identified CD200R1 and CCL19 as unique immunotherapy response markers not previously reported in plasma studies. CD200R1 is a receptor on myeloid/immune cells that transmits inhibitory signals from the CD200 ligand. CCL19 attracts $CCR7^+$ T cells and dendritic cells, with higher expression in the TME correlating with enhanced immune infiltration and better clinical outcomes[33,34]. Their opposing immunological roles point to the complex regulatory balance and underexplored pathways within the TME that shape the response to therapy and influence outcomes.

To extend our findings beyond baseline predictors, we examined circulating markers in 11 patients with matched pre- and post-ICI therapy plasma samples. We identified six markers: CCL21, CD276, IL-2RA, IL-24, IL-1RL1, and AGER, with only IL-2RA having been previously linked to treatment outcome. CCL21, a chemokine involved in lymphocyte trafficking and dendritic cell homing, has not been reported in plasma-based lung cancer studies, though higher plasma levels have been observed in melanoma patients who responded to immunotherapy. CD276, considered an immune checkpoint molecule, was differentially expressed before and after treatment. Torres-Martínez et al. reported significantly higher levels of soluble CD276 in baseline samples of non-responding NSCLC patients by ELISA[35]. IL-24, which has immune-modulatory and tumour-suppressive characteristics, was also differentially expressed, with responders in our cohort showing higher baseline IL-24 compared to non-responders. To our knowledge, no study has compared plasma IL-24 levels before and after immunotherapy. However, Zhang et al. found that IL-24 improved prognosis in NSCLC patients, with serum IL-24 levels negatively correlating with TNM classification, consistent with a tumour-suppressive role in NSCLC[36]. The plasma level of IL-1RL1 was found to have increased at the time of relapse in NSCLC patients with cancer-associated cachexia (CAC) compared with the non-CAC group, showing a negative correlation of this marker within the circulation with the tumour presence[37]. Its reduction in the follow-up samples upon immunotherapy in our cohort is also proving the same trend for this protein.

Finally, we assessed AGER, encoding the Receptor for Advanced Glycation End-products (RAGE), a multiligand pattern-recognition receptor abundantly expressed in lung alveolar cells and involved in inflammation and tissue stress responses. Multiple studies have reported that soluble RAGE negatively correlates with lung cancer, with serum levels decreasing during disease progression[38]. Although we observed a similar trend, none of these studies investigated the impact of immunotherapy on circulating RAGE levels.

Existing predictors of response, such as PD-L1 expression, are inconsistent[10]. By employing a Cox proportional-hazards model on pre-treatment plasma proteomes, alongside the application of the *Stabl* framework to reduce false discoveries from high-plex panels, we identified a four-protein signature for overall survival: CEACAM5, PTX3, FGF23, and AREG. Notably, higher baseline levels of all these proteins predicted worse outcomes in our cohort. CEACAM5, a member of the carcinoembryonic antigen (CEA) family, acts as an oncofetal growth factor and cell-adhesion molecule. Multiple studies have connected higher preoperative or pre-treatment CEA levels with worse prognosis in NSCLC[39]. Dall'Olio et al. further showed that a post-treatment drop in CEA was associated with longer survival under PD-1/PD-L1 therapy[40]. Although some reports differ on how circulating CEA relates to therapy response[41], most available evidence aligns with our findings, showing that higher baseline CEA correlates with greater risk of poor survival[42].

PTX3 (Pentraxin-3) is involved in inflammation and innate immunity, released by myeloid and stromal cells in response to inflammatory cytokines, where it modulates angiogenesis, complement activation, and tissue remodelling. Elevated PTX3 levels, in both tumour tissue and circulation, predict worse overall survival across several malignancies[43]. While PTX3 has not been extensively studied in lung cancer immunotherapy, Diamandis et al. recently found that plasma PTX3 may differentiate lung cancer patients from high-risk smokers with performance comparable to current lung markers[44]. This aligns with our observation that elevated baseline PTX3 predicts poor survival, possibly reflecting a pro-tumour inflammatory environment. FGF23 has not been reported in prior NSCLC plasma proteome studies, nor has its association with survival upon immunotherapy been explored. Although not considered a 'classic' lung cancer marker, higher circulating FGF23 has been linked to shorter overall survival in patients with cancers involving bone metastases[45]. Finally, AREG, an EGF-family ligand and autocrine growth factor that binds EGFR to drive epithelial proliferation, was selected by our model, with overexpression correlating with shorter overall survival in NSCLC patients. AREG is secreted by lung tumour-infiltrating dendritic cells in the tumour microenvironment, promoting cancer cell growth and metastasis[46].

From pre- and post-surgery comparisons to recurrence risk, immunotherapy response, and survival outcomes, our plasma proteomics analysis identified significant biological patterns across the clinical modalities examined, particularly immune-related markers. IL-6, IL-2RA, LAG3, CD276, CCL19, and CCL21 were among the immune-regulatory proteins most frequently selected across models, indicating a broad role of systemic immune regulation in both treatment response and disease progression. In various instances, poorer outcomes were associated with markers such as SPP1 and AREG, which are known to influence immune suppression and tumour–stromal interactions. Strong predictors of survival also included metabolic or checkpoint-related markers like FGF23 and CEACAM5, along with inflammatory mediators such as PTX3. In comparisons between surgery and recurrence, tissue remodelling and extracellular matrix-associated proteins, including THBS3 and CLEC3B, were more prominent, suggesting a potential role for them in micrometastatic activity or tumour resection response. Furthermore, all markers were selected using two statistical models, adaptive Lasso and Stabl, which enhance the likelihood that they are relevant despite the large feature space induced by these high-plex panels. We demonstrated how employing two independent high-dimensional technologies can uncover complementary and therapeutically significant

plasma signals by combining Alamar's NULISAseq platform's ultra-sensitive quantification of low-abundance proteins with SomaScan's extensive proteome coverage. In addition to emphasising immunological and stromal pathways that are common across lung cancer stages, these results collectively provide a foundation for developing reliable blood-based biomarker panels for treatment stratification and personalised therapy.

This study has several limitations to take into consideration. The small sample size may limit the generalisability of these results, particularly when considering recurrence or treatment response groups. Although we utilised complementary proteomics technologies, each has advantages and disadvantages, and variations in target coverage or sensitivity may affect the outcomes, especially when comparing platforms. For instance, the NULISA panel only partially overlaps with the more general SomaScan panel since it mainly focuses on proteins linked to inflammation. We were able to validate a subset of the proteins in a small validation set, but note that a larger validation cohort is needed to fully parse the translatability of these protein signatures as validated biomarkers. Additionally, we studied plasma samples from only two timepoints, before and after surgery and immunotherapy, so we can only get an overview of the changes in protein levels over time. Furthermore, we are unable to directly connect the changes in plasma proteins to the processes occurring within the tumour or its microenvironment, as we did not incorporate corresponding tissue analyses. Lastly, even with the use of well-established normalisation techniques, we may not have been able to completely control variables like sample processing, systemic inflammation, or other medical conditions that could affect plasma protein levels.

Methods

Patient cohort

Ethics approval for this study was obtained from the Metro South Health District Human Research Ethics Committee under the National Health and Medical Research Council guidelines (HREC/11/QPAH/331) to collect samples from the Princess Alexandra Hospital. Patients recruited for this study were treatment-naive and without prior cancer diagnosis within the last 5 years. This study has been ratified by the Queensland University of Technology Human Research Ethics Committee. Patients were grouped based on treatment modality (Fig. 7). Patients who underwent tumour resection surgery ($n = 20$), peripheral blood samples were collected within one week prior to surgery and again 2–4 weeks post-surgery. All patients in this group were enroled with signed informed consent and followed prospectively for clinical outcomes over a period of three to five years. Patients who received immunotherapy (Pembrolizumab, Atezolizumab and Durvalumab), or combination therapy including chemotherapy (Carboplatin, Pemetrexed, Cisplatin, Paclitaxel, Gemcitabine and Docetaxel), targeted therapy (Osimertinib and Crizotinib) and immunotherapy ($n = 36$), blood samples were collected at baseline (on the day of or the day before the first round of systemic therapy) for 25 patients, and at baseline and 3–6 months after treatment initiation for 11 patients. Patient responses to immunotherapy were assessed based on RECIST 1.1 criteria. All participants were recruited from the Princess Alexandra Hospital thoracic and lung cancer clinic between March 2019 and August 2024.

The validation cohort consisted of 114 NSCLC patients recruited from the Princess Alexandra Hospital lung cancer clinic, comprising 107 baseline and 5 follow-up samples from 108 patients treated with surgical resection. Tumour recurrence information was available for 12 patients with baseline measurements. An additional 6 patients treated with immunotherapy agents and no surgical resection were added, with progression-free survival and overall survival information available.

Blood sample processing

Patient blood samples were collected using K_2EDTA-coated tubes (BD Diagnostics, US) and immediately mixed. Plasma separation was completed within 4 h of collection by centrifugation at 2200 × *g* for 15 min at 4 °C with the break off. The samples were then aliquoted and stored at −80 °C prior to blood proteomic profiling.

Blood proteomic profiling of NSCLC plasma samples using SomaScan

Matched plasma samples from 20 patients pre- and post-tumour resection (40 samples in total, 55 µL/sample) were profiled using the SomaScan v4.1 assay. Plasma was analysed using a protein panel with 7596 SOMAmers (7301 have available UniProt IDs and some target same proteins). Samples were randomised and ran on 96-well plates alongside external control samples (calibrators, quality control (QC), and buffer). Serial dilutions (0.05%, 0.5%, and 20%) were used to optimise the detection of protein targets, with the full panel of SOMAmers present in all dilutions, a design consistently applied across all samples. Raw data were standardised using external control samples to adjust for variability in microarrays and discrepancies both within and between plates. This process included adaptive normalisation by maximum likelihood (ANML) to an external reference, aimed at reducing inter-sample variability. The final SomaScan data provided in ANML format in relative fluorescence units (RFU) were log-transformed (log-2) for the main analysis. The limit of detection (LOD) for each SOMAmer was determined using external buffer samples. Where multiple measurements were taken when the same protein was measured by different probes, the median values were taken per patient, or mean values when only two were available. Quality control was performed by comparing the median of QC samples on each plate to the reference, and a cross-plate QC check measure (pass/flag) was assigned to each SOMAmer.

Nucleic acid linked immuno-sandwich assay (NULISA)

NULISA **is** a fully automated platform designed for multiplex proteomic assays, was used to analyse 25 baseline samples collected before immunotherapy, 11 baseline samples and their matched post-immunotherapy counterparts (22 samples in total), and 17 paired samples collected before and after tumour resection surgery, all of which were matched with the SomaScan assay. Plasma was run on the NULISA inflammation Panel 250. Briefly, immunocomplexes were formed using paired oligonucleotide-conjugated antibodies, followed by sequential capture steps with oligo-dT and streptavidin beads, ligation of DNA reporters, and barcoding of samples. The resulting libraries, comprising both target- and sample-specific molecular identifiers, were PCR-amplified, purified, and sequenced using the AVITI platform (Element Biosciences). Each run incorporated multiple layers of quality control, including internal controls (exogenous spike-ins) to normalise individual sample counts, pooled plasma controls to assess intra- and inter-plate consistency, and negative controls (assay buffer only) to evaluate background signal and determine the limits of detection (LOD). Data normalisation followed a multi-step process: raw target counts were first divided by the internal control counts for each sample, then normalised to the median of the inter-plate control for each target and scaled by a factor of 10^4. A pseudo-count of +1 was added prior to log2 transformation. The final output, expressed as NULISA Protein Quantification (NPQ) units, reflects log2-normalised protein expression levels. Plate-specific LODs were determined by calculating the mean value plus three standard deviations of the untransformed signal from the negative controls, followed by the same normalisation and log transformation steps. To ensure data quality, any sample with internal control values deviating by more than ±40% from the plate-wide median was flagged for further evaluation. These samples underwent additional assessment using downstream dimensionality reduction techniques, including principal component analysis and heatmap clustering, to determine their suitability for inclusion in the final dataset.

Next-generation enzyme-linked immunosorbent assays (nELISA)

Circulating protein levels were measured using the Nomic Bio high-throughput proteomics platform, which quantified 973 circulating proteins per sample, including cytokines, soluble receptors, growth factors, proteases, and toxicity markers. Plasma samples from the validation cohort were analysed using standard protocols, as described previously[47]. Briefly, nELISA pre-assembles antibody pairs on spectrally encoded microparticles, creating spatial separation between non-cognate antibodies to prevent

reagent-driven cross-reactivity while enabling multiplexing of hundreds of ELISAs in parallel using flow cytometry. Standard curves were included for each protein, enabling absolute quantification in pg/mL concentrations. This orthogonal platform was selected for validation as it provides antibody-based quantification (unlike aptamer-based SomaScan) with broader coverage than NULISA and gold-standard ELISA quantification.

Statistical analysis

We used a multitiered statistical framework, including descriptive statistics, univariate tests, and false discovery-corrected feature selection. For feature selection, we used adaptive Lasso (ALasso) regression within the Stabl algorithm, a method established by SurgeCare[14], and standard stability selection using ALasso[48,49]. Stabl is a statistical framework that uses artificial feature injection, stability-based feature selection, and false discovery control of a false discovery proportion (FDP) estimate to find reliable sets of predictive biomarkers from high-dimensional datasets. The final fits to the selected markers were varied on the relevant sample subset and ranged from unweighted Logistic Regression models to Ridge-Regression models and l1-weighted Cox Proportional Hazards models. In each pseudo-experiment, data were randomly subsampled, artificial features were created using random permutation, and false discovery rates of uninformative features were estimated using these artificial features. Cross-validation was done using a robust Monte Carlo 5×5 method, with stratification by patient ID to prevent data leakage and to preserve the integrity of comparisons between matched samples from the same patient. The feature selection and the choice of a stability threshold of Stabl were adjusted by evaluating several parameters, such as the final regression regularisation parameters, artificial feature generation approach, and, where false-discovery control failed, signal-to-noise ratio. For each comparison modality, the most stable features, defined as those exceeding the optimised data-driven selection frequency threshold and for which the associated model achieved statistical significance in predictions ($P < 0.05$), were retained. The area under the receiver operating characteristic curve (AUROC) was used to evaluate the predictive performance of the models. To account for multiple comparisons in the pathway analysis, p-values ($p < 0.05$) were adjusted using an FDR correction. K-fold tests in the survival analysis to predict patient response were conducted with four folds and ten repeats. Correlation analysis was performed on matched plasma samples examined via both the SomaScan and NULISA platforms. Shared markers consistent across both assays were chosen, and the Pearson correlation of expression levels was clustered using the distance metric to assess regions of cross-platform panel correlation.

Validation study

To validate the key findings from the discovery arm of the study, we analysed both an independent and the internal cohorts of NSCLC patients using the nELISA platform. Statistical analysis of differentially expressed proteins in the validation analyses utilised the *limma* package. Survival and Cox Proportional Hazards (CoxPH) analysis of selected proteins utilised *lifelines* with patient age, sex, and adenocarcinoma vs. other histology as covariates to model overall survival[50].

Data availability

The datasets generated and/or analysed during the current study are not publicly available due to patient-level information and are subject to confidentiality. De-identified data are available from the corresponding author on reasonable request.

Received: 14 July 2025; Accepted: 29 April 2026;
Published online: 12 May 2026

References

1. Siegel, R. L., Miller, K. D. & Jemal, A. Cancer statistics. *CA Cancer J. Clin.* **70**, 7–30 (2020).
2. Zhou, J. et al. Global burden of lung cancer in 2022 and projections to 2050: Incidence and mortality estimates from GLOBOCAN. *Cancer Epidemiol.* **93**, 102693 (2024).
3. Crosby, D. et al. Early detection of cancer. *Science* **375**, eaay9040 (2022).
4. Albanes, D. et al. The blood proteome of imminent lung cancer diagnosis. *Nat. Commun.* **14**, 3042 (2023).
5. Rathod, R. et al. Factors influencing false positive low-dose computed tomography-based lung cancer screening in an urban, safety-net system. *Cancer Res.* **85**, 7408–7408 (2025).
6. Patz, E. F. et al. Overdiagnosis in low-dose computed tomography screening for lung cancer. *JAMA Intern. Med.* **174**, 269–274 (2014).
7. Mehan, M. R. et al. Protein signature of lung cancer tissues. *PLoS ONE* **7**, e35157 (2012).
8. Macklin, A., Khan, S. & Kislinger, T. Recent advances in mass spectrometry based clinical proteomics: applications to cancer research. *Clin. Proteom.* **17**, 17 (2020).
9. Zhao, R. et al. Plasma proteomic profiles for early detection and risk stratification of non-small cell lung carcinoma: A prospective cohort study with 52,913 participants. *Int. J. Cancer* **157**, 1577–1589 (2025).
10. Bar, J. et al. Biological insights from plasma proteomics of non-small cell lung cancer patients treated with immunotherapy. *Front. Immunol.* **ume 15**, 2024 (2024).
11. Tognetti, M. et al. Biomarker candidates for tumors identified from deep-profiled plasma stem predominantly from the low abundant area. *J. Proteome Res.* **21**, 1718–1735 (2022).
12. Geyer, P. E. et al. The circulating proteome—Technological developments, current challenges, and future trends. *J. Proteome Res.* **23**, 5279–5295 (2024).
13. Yaghoubi Naei, V. et al. Advances in novel strategies for isolation, characterization, and analysis of CTCs and ctDNA. *Ther. Adv. Med. Oncol.* **15**, 17588359231192401 (2023).
14. Hédou, J. et al. Discovery of sparse, reliable omic biomarkers with Stabl. *Nat. Biotechnol.* **42**, 1581–1593 (2024).
15. Wu, W. et al. IL-2Rα-biased agonist enhances antitumor immunity by invigorating tumor-infiltrating CD25+CD8+ T cells. *Nat. Cancer* **4**, 1309–1325 (2023).
16. Lin, X. et al. Regulatory mechanisms of PD-1/PD-L1 in cancers. *Mol. Cancer* **23**, 108 (2024).
17. Raffield, L. M. et al. Comparison of proteomic assessment methods in multiple cohort studies. *Proteomics* **20**, 1900278 (2020).
18. Baker, K. J. et al. IL-36 expression is increased in NSCLC with IL-36 stimulation of lung cancer cells promoting a pro-tumorigenic phenotype. *Cytokine* **165**, 156170 (2023).
19. Kimura, Y. et al. Serum CA125 level is a good prognostic indicator in lung cancer. *Br. J. Cancer* **62**, 676–678 (1990).
20. Nakamura, H. & Nishimura, T. History, molecular features, and clinical importance of conventional serum biomarkers in lung cancer. *Surg. Today* **47**, 1037–1059 (2017).
21. Ly, D. et al. Role for high-affinity IgE receptor in prognosis of lung adenocarcinoma patients. *Cancer Immunol. Res.* **5**, 821–829 (2017).
22. Liang, Y. et al. The increased expression and aberrant methylation of SHC1 in non–small cell lung cancer: Integrative analysis of clinical and bioinformatics databases. *J. Cell Mol. Med.* **25**, 7039–7051 (2021).
23. Bertoglio, P. et al. EP07.04-19 clinical and molecular profile and risk factors of stage IA NSCLC relapsing after radical resection. *J. Thorac. Oncol.* **18**, S552–S553 (2023).
24. Schuurbiers, M. M. F. et al. Recurrence prediction using circulating tumor DNA in patients with early-stage non-small cell lung cancer after treatment with curative intent: a retrospective validation study. *PLOS Med.* **22**, e1004574 (2025).
25. Hollinshead, K. E. et al. Respiratory supercomplexes promote mitochondrial efficiency and growth in severely hypoxic pancreatic cancer. *Cell Rep* **33**, 108231 (2020).

26. Wang, Y. et al. Nebulized inhalation of extracellular vesicles containing SPOCK2 suppresses lung adenocarcinoma progression via MAPK inhibition. *Discov. Oncol.* **16**, 1–14 (2025).
27. Chen, J. et al. Enhanced expression of FGF19 predicts poor prognosis in patients with non-small cell lung cancer. *J. Thorac. Dis.* **13**, 1769 (2021).
28. Naqash, A. R. et al. Increased interleukin-6/C-reactive protein levels are associated with the upregulation of the adenosine pathway and serve as potential markers of therapeutic resistance to immune checkpoint inhibitor-based therapies in non-small cell lung cancer. *J. Immunother. Cancer* **11**, e007310 (2023).
29. Siemiątkowska, A. et al. Serum sCD25 protein as a predictor of lack of long-term benefits from immunotherapy in non-small cell lung cancer: a pilot study. *Cancers* **13**, 3702 (2021).
30. Ramoni, D. et al. Circulating osteopontin predicts clinical and radiological response in first-line treatment of advanced non-small cell lung cancer. *Lung* **202**, 197–210 (2024).
31. Kang, D. H. et al. Baseline serum interleukin-6 levels predict the response of patients with advanced non-small cell lung cancer to PD-1/PD-L1 inhibitors. *Immune Netw.* **20**, e27 (2020).
32. Su, S. et al. Predictive value of peripheral blood biomarkers in patients with non-small-cell lung cancer responding to anti-PD-1-based treatment. *Cancer Immunol. Immunother.* **73**, 12 (2024).
33. Gu, Q. et al. CCL19: a novel prognostic chemokine modulates the tumor immune microenvironment and outcomes of cancers. *Aging* **15**, 12369–12387 (2023).
34. Shao, A. & Owens, D. M. The immunoregulatory protein CD200 as a potentially lucrative yet elusive target for cancer therapy. *Oncotarget* **14**, 96–103 (2023).
35. Torres-Martínez, S. et al. Circulating immune proteins: improving the diagnosis and clinical outcome in advanced non-small cell lung cancer. *Int. J. Mol. Sci.* **24**, 17587 (2023).
36. Zhang, K. et al. Serum IL-24 combined with CA125 as screening and prognostic biomarkers for NSCLC. *Cell Biol. Int.* **48**, 1160–1168 (2024).
37. Al-Sawaf, O. et al. Body composition and lung cancer-associated cachexia in TRACERx. *Nat. Med.* **29**, 846–858 (2023).
38. Jing, R. et al. Receptor for advanced glycation end products (RAGE) soluble form (sRAGE): a new biomarker for lung cancer. *Neoplasma* **57**, 55 (2010).
39. Duan, F. et al. A novel diagnostic model for predicting immune microenvironment subclass based on costimulatory molecules in lung squamous carcinoma. *Front. Genet.* **ume 13**, 2022 (2022).
40. Dall'Olio, F. G. et al. CEA and CYFRA 21-1 as prognostic biomarker and as a tool for treatment monitoring in advanced NSCLC treated with immune checkpoint inhibitors. *Ther. Adv. Med. Oncol.* **12**, 1758835920952994 (2020).
41. Dal Bello, M. et al. The role of CEA, CYFRA21-1 and NSE in monitoring tumor response to Nivolumab in advanced non-small cell lung cancer (NSCLC) patients. *J. Transl. Med.* **17**, 1–10 (2019).
42. Marin-Acevedo, J. A., Kimbrough, E. O. & Lou, Y. Next generation of immune checkpoint inhibitors and beyond. *J. Hematol. Oncol.* **14**, 45 (2021).
43. Jung, H. et al. Prognostic value of pentraxin3 protein expression in human malignancies: a systematic review and meta-analysis. *Cancers* **16**, 3754 (2024).
44. Diamandis, E. P. et al. Pentraxin-3 is a novel biomarker of lung carcinoma. *Clin. Cancer Res* **17**, 2395–2399 (2011).
45. Mansinho, A. et al. Levels of circulating fibroblast growth factor 23 (FGF23) and prognosis in cancer patients with bone metastases. *Int. J. Mol. Sci.* **20**, 695 (2019).
46. Hsu, Y. L. et al. Lung tumor-associated dendritic cell-derived amphiregulin increased cancer progression. *J. Immunol.* **187**, 1733–1744 (2011).
47. Dagher, M. et al. nELISA: a high-throughput, high-plex platform enables quantitative profiling of the inflammatory secretome. *Nat. Methods* **22**, 2375–2385 (2025).
48. Meinshausen, N. & Bühlmann, P. Stability selection. *J. R. Stat. Soc. Ser. B Stat. Methodol.* **72**, 417–473 (2010).
49. Zou, H. The adaptive lasso and its oracle properties. *J. Am. Stat. Assoc.* **101**, 1418–1429 (2006).
50. Davidson-Pilon lifelines: survival analysis in Python. *J. Open Source Softw.* **4**, 1317 (2019).

Acknowledgements

This study was supported by the Frazer Institute (University of Queensland), Queensland Spatial Biology Centre (Wesley Research Institute), the Harding Family Fellowship, Cure Cancer, and the PA Research Foundation. The authors acknowledge the Alamar Biosciences, Nomic Bio, and Somalogic technology access programs.

Author contributions

Concept: M.A., M.E.W., and A.K. Experimentation: V.Y.N., S.D., C.O., W.M., J.M.1, and K.O.B. Data analysis: C.Y.N., A.K.1, A.W.Y., C.L., J.H., and G.M. Writing and critical review: all authors.

Competing interests

J.H. is a director and G.M. an employee of SurgeCare, SAS. J.M. is an employee of Standard Biotools. A.K. is on the Scientific Advisory Board for Omapix Solutions, Predxbio, Molecular Instruments, Lumito and Visiopharm. All other authors declare no cometing interests.

Additional information

Supplementary information The online version contains supplementary material available at https://doi.org/10.1038/s41698-026-01469-z.

Correspondence and requests for materials should be addressed to Arutha Kulasinghe.

Reprints and permissions information is available at http://www.nature.com/reprints

Publisher's note Springer Nature remains neutral with regard to jurisdictional claims in published maps and institutional affiliations.

Open Access This article is licensed under a Creative Commons Attribution-NonCommercial-NoDerivatives 4.0 International License, which permits any non-commercial use, sharing, distribution and reproduction in any medium or format, as long as you give appropriate credit to the original author(s) and the source, provide a link to the Creative Commons licence, and indicate if you modified the licensed material. You do not have permission under this licence to share adapted material derived from this article or parts of it. The images or other third party material in this article are included in the article's Creative Commons licence, unless indicated otherwise in a credit line to the material. If material is not included in the article's Creative Commons licence and your intended use is not permitted by statutory regulation or exceeds the permitted use, you will need to obtain permission directly from the copyright holder. To view a copy of this licence, visit http://creativecommons.org/licenses/by-nc-nd/4.0/.

© The Author(s) 2026